Structural investigation on Silicate Mica Glass Ceramics

Ola N. Megahed [*1], *Naer A. Baker* [1], *Maysa I. Abdelhamid* [1] *&Noha A. El-Wassefy* [2]

1. Physics Department, Faculty of science, Mansoura University, Egypt

2 Faculty of Dentistry, Mansoura University, Egypt. ***Correspondence to: O.N. Megahed;***
olanagymegahed@gmail.com

Abstract: The present work deals with the preparation and characterization of mica glass ceramic (MGC) under the effect of controlled heat treatment. A hydrothermal method was used to prepare this powdered sample. Differential scanning analysis (DSC), Heat treatment (HT), Fourier transform infrared (FTIR) spectroscopy, X-ray diffraction (XRD) spectroscopy and ^{27}Al and ^{29}Si NMR spectroscopy were used to examine the structural features of the samples. The main goal of this research is to develop an amorphous glass that can be turned into glass ceramic by using controlled thermal heat treatment process. Furthermore, we provide a potential method for converting glass ceramics into glass ionomer cement (GIC) using acid-base reaction process. Separation of the carboxylic cemented species from the host matrix is the main goal, which was detected by FTIR spectroscopy. The other techniques were used to Know more information about the produced powder. We also, study the effect of addition of ZnO and ZrO_2 to the glass powder with FTIR and DFT techniques to know their structural role.

keywords: Mica Glass ceramic (MGC), NMR Spectroscopy, Glass ionomer cement (GIC)

1. INTRODUCTION

1.1 General background

Mica glass ceramics (MGCs) are inorganic sort of specific types of oxide glasses [1-6]. Simply they are composed of aluminum hydrous silicate, potassium, sodium, and trace amounts of a variety of additional elements such as TiO_2 or ZnO. The Mica glasses are most commonly found as the crystalline potassium aluminum silicate mineral KAl_2 $(AlSi_3O_{10})$ $(OH)_2$. The inorganic material with a specification of (MGC) has easy controlled volume nucleation and crystallization, making it suitable for biomedical applications such as teeth restoration [6-10]. Mica crystals have a low ratio to the extra phases dispersed in the ceramic material's matrix. MGC is the most popular mineral for usage in a variety of industries as well as for personal consumption due to its high silica concentration. It's almost always utilized as fillers and extenders, as well as offering better uniformity, improved workability, and crack prevention [4-8].

Each element that makes up the MGCs matrix has a distinct role in strengthening the structure and in the characteristics of the MGC [5-9]. Titanium oxide (TiO_2), for example, can only be used as a white opacifier at low concentrations. In dental mica glass ceramics, ZnO is a desired opacifier. This is in addition to its function as a factor in chemical resistance and fluxing power. Aluminum oxide (Al_2O_3) improves the material strength and hardness [4,7,9] while also preventing fracture spread through the surface or in the bulk. Calcium and phosphors improve the bioactivity and compatibility of the material. An excellent Glass ceramic (GC) [11-14] is applied in the field of glass ionomer cements (GIC) that having the characteristics mentioned above [15,16]. Dental cements based on GIC are made up of three chemically distinct materials which are an organic matrix or organic phase, an inorganic matrix called filler or disperse phase containing wollastonite species ($CaSiO_3$) as the filler, and an organosilane or coupling agent to bond the filler to the organic resin [17].

The goal of this research is to develop an amorphous glass that can be turned into glass

ceramic using thermal heat treatments processes Furthermore, we provide a potential method for converting GC into GIC using acid-base reaction process. Separation of the carboxylic cemented species from the host matrix is the main goal.

2. Materials and Methods

2.1. Materials Preparation

The precursors used in this method were calcium nitrate tetrahydrate, ammonium hydrogen phosphate and sodium hydroxide solution for CaO, P_2O_5 and Na_2O respectively. The additional oxides such as Al_2O_3, and TiO_2 precursors were dissolved in de-ionized water, mixed with SiO_2 at mole percent (mol %) varying from 40 % to 60 % and transferred to an electrical shaker for 1 hour. Then, the mixture was transferred to a water bath at 80 ℃ for 8 days. The obtained powder was washed in de-ionized water, filtered and dried in an oven at 100 ℃.

2.2. Experimental techniques

2.2.1 Differential Scanning Calorimetry (DSC) analysis

Differential scanning calorimetry (DSC) is a universal technique for thermal analysis that measures the amount of heat absorbed or released by a sample as a function of temperature.

The thermal experiment of two selected samples was carried out to obtain the glass transition temperature (T_g) and crystallization peak temperature (T_c) in order to choose a precise temperature for thermal treatment of some samples.

2.2.2 Heat Treatment (HT)

The as prepared sample was firstly dried at 100 ℃ and then treated at temperature in a muffle furnace (Heraeus KR170) with controlled within ± 2 °C. The samples were heat-treated at a temperature (950 ℃) according to the DSC curve which is represented in the Figure (1). After heating was done, the sample were kept into the furnace and held at the temperature of heat treatment (950 ℃) for the desired time (6 h) before the sample was allowed to cool normally at room temperature.

2.2.3 X-ray Diffraction Spectroscopy (XRD)

Shimadzu X-ray diffract meter was used for the X-ray diffraction measurements (the apparatus type Dx-30, Metallurgy institute, El Tebbin-Cairo). The maximum peak and the intensity values were used to determine the type of the material that compared to the patterns in joint committee for powder diffraction standards' international powder diffraction file (PDF) database (JCPDS).

2.2.4 Nuclear Magnetic Resonance (NMR) Measurements

Nuclear Magnetic Resonance (NMR) spectra of the powdered samples were recorded at room temperature using a JEOL GSX-500 high-resolution solid state MAS NMR spectrometer with a magnetic field of 11.74 T (Mansoura University-EGYPT). The ^{29}Si and ^{27}Al MAS NMR spectra were measured at 59.63 and 78.20 MHz respectively. The samples were rotated about the 'magic angle' at a rate of 6 kHz for ^{29}Si and ^{27}Al spectra. These rates are sufficient to remove the spinning sidebands from the true peaks. The ^{27}Al MAS NMR spectra were assigned to two overlapping resonances whose chemical shift values were evaluated. But such results can only be employed qualitatively, because a certain fraction of the quadrupole nuclei may escape observation, and the data suffer from systematic errors. The accuracy of the chemical shift measurements in these glasses is not better than ± 1 ppm.

### 2.1.5 Fourier Transform Infrared (FTIR) Spectroscopy

Fourier transform infrared (FTIR) absorption spectroscopy for different samples were carried out by means of potassium bromide (KBr) pellets technique. The spectra were measured in the region of (400 – 4000) cm^{-1} with a spectral resolution of 2 cm^{-1} by using a Mattson 5000 FTIR spectrometer. The resulted spectrum was normalized to the spectrum of blank (KBr) pellet and were corrected to the background and dark currents by using two-point baseline correction. The normalization is required to eliminate the effect of concentration of the powder sample in the (KBr) disc.

3. Results and discussion

3.1 DSC analysis

Figure (1) shows the DSC curve of silicate powder modified with calcium, sodium, phosphors, aluminum and titanium oxide. The curve provides a T_c from 900 to 1100 °C.

According to the exothermic peak in the DSC curve, the sample was treated at 950 °C for 6 h.
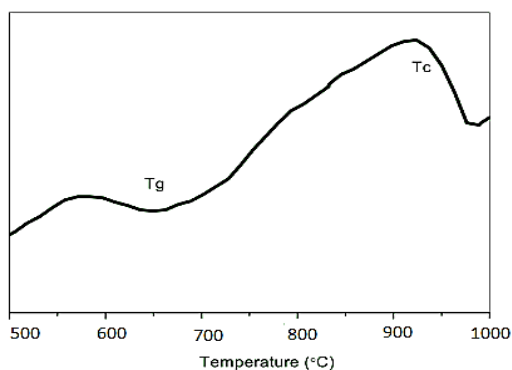
Figure (1). DSC curve of silicate powder modified with calcium, sodium, phosphors, aluminum and titanium oxide.

3.2 XRD analysis

The sample dried at 100 °C and the thermally treated sample were checked by XRD spectroscopy technique. **Figure (2a)** shows the XRD spectra of the as obtained glass dried at 100°C. **Figure (2b)** shows the XRD of sample treated at 950 °C for 6 h.
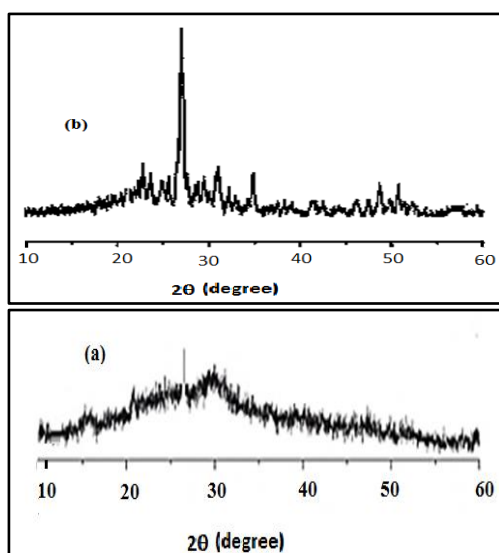

Figure (2). (a) XRD spectra of the as obtained glass dried at 100°C and (b) Sample treated at 950 °C for 6 h.

The XRD of the studied compositions have presented the anorthite phase ($CaAl_2Si_2O_8$) (86-1706Ca ($Al_2Si_2O_8$)) [17-19] when they were heat-treated at 950 °C for 6 h. However, an amorphous structure predominates in the dried sample at 100 °C, confirming that the irregular structure of the glass. On the other side, for the heat-treated material at 950 °C, it displays defined peaks characteristic of the anorthite crystalline structure [18,19], which is a useful derivative for mica glass ceramic (MGC).

3.3 NMR analysis

The data based on XRD is further confirmed by ^{29}Si NMR spectra of the sample treated at 950 °C, as shown in Figure (3). It can be shown from the figure that, there are two separated resolved resonance peaks, one located at (-88) ppm and related to silicate units of (Q^3) coordination (silicate unit with three bridging oxygen BO, bonds). This means that SiO_2 unit contains three bridging oxygen atoms (BO). One of such bonds is connected between Si and Al and there is only one non-bridging oxygen (NBO) atom compensated with $Ca.^{2+}$ The accumulation of such species ($CaAl_2Si_2O_8$) is the main reason for appearing the line spectra located at (-88) ppm. There is another broader peak at about (-70) ppm which is related to silicate structural units containing high concentration from non-bridging bonds (NBO).
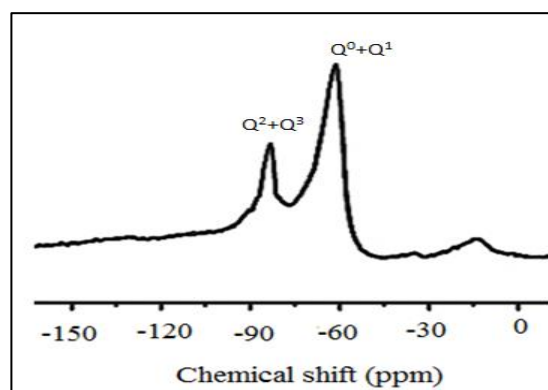
**Figure (3).** ^{29}Si NMR spectra of sample treated at 950°C.

The results based on ^{29}Si NMR spectroscopy is agreed with that obtained from ^{27}Al NMR spectroscopy as in Figure (4). The ^{29}Si MAS NMR spectra show splitting into individual lines. Each one has a specific value of chemical shift that characterizes a silicate structural species. The ^{27}Al MAS NMR spectra were assigned to overlapping resonances whose chemical shift values were evaluated. But such results can only be employed qualitatively to separate each resonance from the whole spectra.
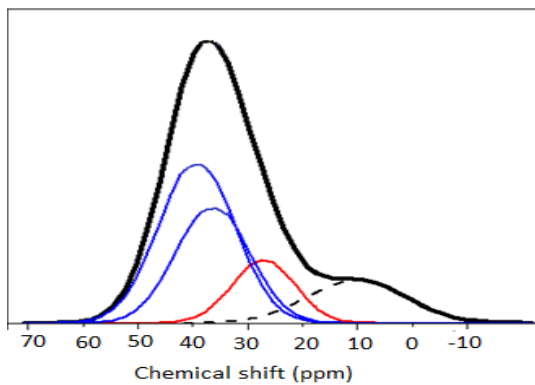
Figure (4). ^{27}Al NMR spectra of sample treated at 950 °C.

The spectra appeared in Figure (4) involves resonance limes. The resonance of peak centered at (43) ppm is assigned to tetrahedral aluminum (AlO$_4$) coordinated contain two NBO and the other oxygen atoms are bridged with Si atom. This means that (Si-O-Al) bond is present. The band centered about (28) ppm is the tetrahedral aluminum of three NBO and compensated Ca^{+2} ions. The broad bands with peak centered at (5) ppm is due to species connected with orthophosphate units. The above arguments support that Al is considered as a central atom surrounded with Si and P as a second neighbors. This attribution leads to expect that anorthite phase (CaAl$_2$Si$_2$O$_8$) should be formed in such materials [1-6].

3.4 FTIR analysis
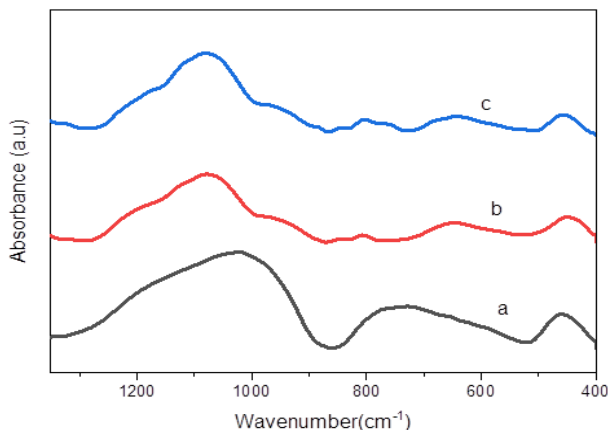
Figure (5). FTIR absorbance spectra for the modified silicate glass composition, (a) free glass sample, (b) sample containing 1 mol% ZnO and 4 mol% ZrO$_2$ and (c), sample containing 4 mol% ZnO and 1 mol% ZrO$_2$.

FTIR absorption spectra for the modified silicate glass compositions are shown in Figure (5). The obtained spectra of the composition (ZnO+ZrO$_2$) (curve b, c) and the free glass (curve a) involves three separated strong bands. The first broad band ranged from (400-520) cm^1, is assigned to cationic vibration like Na$^+$ and Ca^{+2} in the Phosphate and silicate structural units. The second one between (520-820) cm^1, is assigned to (Si-O) vibration in silicate units. The band between (550-870 cm^{-1}), is assigned (Si-O) bending NBO in (Q^o) silicate units. However, the absorption band in the region (920-1350 cm^{-1}) is assigned to (Si-O) vibrations modes in the silicate units containing mixed species from three and two bridging oxygen (Q^3 and Q^2). This assignment is consistent with the IR spectra computed by using accurate calculations obtained from deconvolution of Fourier transformation spectra (DFTs), (Figures 6-8).

It can also realize from Figure (5) that the spectra of (ZnO+ZrO$_2$) containing glasses (b and c) are differed from that of glass free from them (curve a). The peaks centered at about (700 and 1000) cm^{-1} are highly decreased and shifted toward a higher wavenumber upon presence of ZnO and ZrO$_2$. This change leads to confirm that the concentration of NBO in both (Q^o) and (Q^1) is decreased and the most dominant species are found in (Q^2) units represented by the peak centered on around (1050) cm^{-1}. Decreasing NBO in the glass upon addition of Zn^{+2} and Zr^{+4} leads that portion from them can enter the glass as glass formers (ZnO and ZrO$_2$). Formation of such latter species required modifier oxide that should be withdrawn from silicate structural units (Q^o and A1). As a result (Q^2) is alternatively the more formed units.
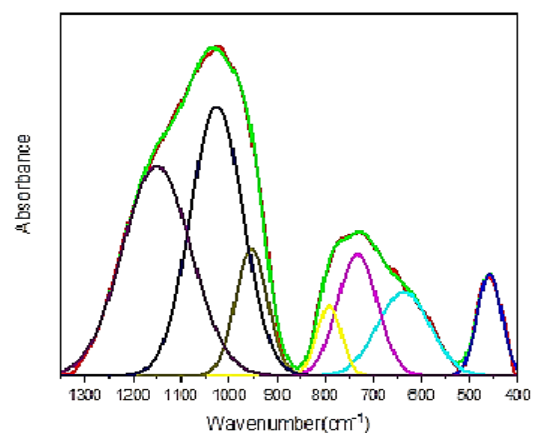
Figure (6). DFTs of the prepared sample without any additions of ZnO or ZrO$_2$.
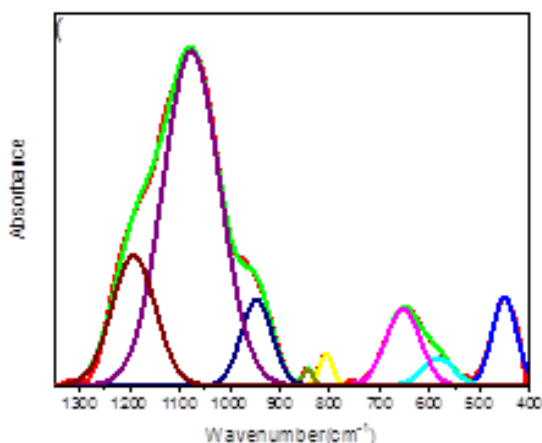
Figure (7). DFTs of the sample containing 1 mol% ZnO and 4 mol% ZrO_2.
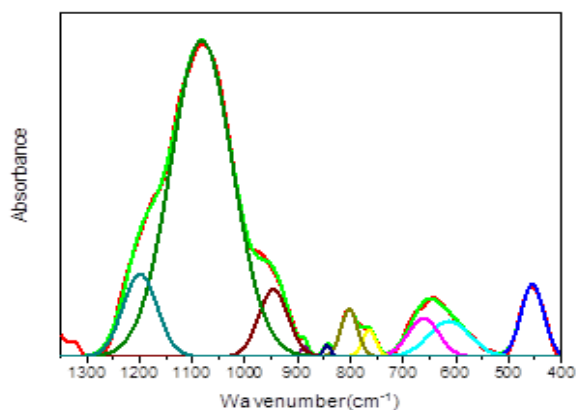
Figure (8). DFTs of the sample containing 4 mol% ZnO and 1 mol% ZrO_2.

The relative areas (RA) representing each units (Q^o, Q^1 and Q^2+Q^3) can be obtained from deconvolution process for FTIR spectra, Figures (6-8). The obtained values for each species are listed in the Table (1). The spectra of samples containing ZnO and ZrO_2 showing clears changes when compared with sample free from them. Figures (7, 8) showed FTIR specter for samples containing 5 mol% (ZnO+ZrO_2). In both two compositions, the concentration of NBO is decreased when the sample is modified by ZnO and ZrO_2. Decreasing NBO is referred to the dual structural role of ZnO and ZrO_2, since they entered as glass former.

It can be seen from the figure that the absorbance peak between (500-750) cm^{-1} referred to (Q^o) is reduced when it compared with that of the as obtained sample (Figure (6)). In addition, a new peak is appeared between (850-100 cm^{-1}) which referred to (Q^1).Then an addition of ZnO and ZrO_2 cause a reduction in (Q^o) and units due to its transformation to (Q^2) (peak centered at 1050 cm^{-1}). In this situation

(Q^2) is the more structural units in the host silicate network. An additional peak representing (Q^3) centered on around (1230) cm^{1}can also observed.

Table (1): The relative areas representing each unit (Q^o, Q^1 and Q^2+Q^3) from the deconvolution process of FTIR spectra.

Position	RA (Free ZnO+ZrO$_2$)	RA (4 ZnO + 1 ZrO$_2$)	RA (4 ZrO$_2$ +1 ZnO)
(400-500) cm^{-1} (Q^o)	0.1	0.04	0.03
(500-850)(Q^o+Q^1)	0.27	0.12	0.11
(850-1300) (Q^2+Q^3)	0.63	0.84	0.86

4. Conclusion

We can successfully prepare a glass sample by hydrothermal method then converting it into mica glass ceramic (MGC) by using the controlled heat treatment (950℃) which known from DSC curve.

The amorphous nature of glass was confirmed by XRD technique and the controlled crystallinity of MGC was also confirmed by this technique.

Addition of ZnO and ZrO_2 to the glass, confirm that the concentration of NBO in both (Q^o) and (Q^1) is decreased and the most dominant species are found in (Q^2) units. While, decreasing NBO in the glass upon addition of Zn^{+2} and Zr^{+4} leads that portion from them can enter the glass as glass formers (ZnO and ZrO_2).

5. Acknowledgments

6. References

1. Goel A., A.A. Reddy, M.J Pascual, L. Gremillard, A. Malchere, J.M. Ferreira, (2012), Sintering behavior of lanthanide-containing glass-ceramic sealants for solid oxide fuel cells, *J. Mater. Chem.*, **22,** 10042-10054.
2. Reddy A.A., D.U Tulyaganov, A. Goel, M. Sardo, P.V. Wiper, M.J. Pascual, V.V. Kharton, V.A. Kolotygin, E.V. Tsipis, L. Mafra, J.M. Ferreira, Melilite glass–(2013),ceramic sealants for solid oxide fuel cells: effects of ZrO_2 additions assessed by microscopy, diffraction and

solid-state *NMR, J. Mater. Chem.*, **1**, 6471− 6480.

3. Tulyaganov D.U., A.A. Reddy, V.V. Kharton, J. M. Ferreira, (2013), Aluminosilicate-based sealants for SOFCs and other electrochemical applications− A brief review, *J. Power Sources*, **242**, 486−502.

4. Reddy A.A., D.U. Tulyaganov, V.V. Kharton, J.M. Ferreira, (2015), Development of bilayer glass-ceramic SOFC sealants via optimizing the chemical composition of glasses—a review, *J. Solid State Electrochem*, , **19**, 2899−2916.

5. Mahapatra M.K., K. Lu, (2010), Seal glass for solid oxide fuel cells, *J. Power Sources*, **195**, 7129−7139.

6. Mahapatra M.K., K. Lu (2010), Glass-based seals for solid oxide fuel and electrolyzer cells–a review, *J. Mater. Sci. Eng.,* **67**, 65−85.

7. Lee S.K., H.I. Kim, E.J. Kim, K.Y. Mun, S. Ryu, (2016), Extent of disorder in magnesium aluminosilicate glasses: Insights from 27Al and 17O NMR, *J. Phys. Chem.*, **120**, 737−749.

8. Henderson G.S., G. Calas, J.F. Stebbins, (2006), The structure of silicate glasses and melts, Elements**2**, 269−273.

9. Fergus J.W., (2005), Sealants for solid oxide fuel cells. *J. Power Sources***147**, 46-57.

10. Kharton V., M.F. José, M.F. Ferreira, (2017), Understanding the formation of $CaAl_2Si_2O_8$ in melilite-based glass-ceramics: combined diffraction and spectroscopic studies, *ACS Omega*, **2,** 6233−6243.

11. Marques V.M.F., D.U. Tulyaganov, S. Agathopoulos, V.K. Gataullin, G.P. Kothiyal, J.M. Ferreira, (2006), Low temperature synthesis of anorthite based glass-ceramics via sintering and crystallization of glass-powder compacts, *J. Eur. Ceram. Soc.*, **26**, 2503−2510.

12. Guignard M., L. Cormier, Environments of Mg and Al in $MgO–Al_2O_3–SiO_2$ 2008, glasses: A study coupling neutron and X-ray diffraction and Reverse Monte Carlo modeling, *Chem. Geol.*, 256, 111−118.

13. Padture N.P., H.M. Chan, 1992, On the constrained crystallization of synthetic anorthite ($CaO^. Al_2O_3^. 2SiO_2$). *J. Mater. Res*, **7**, 170-177.

14. El Damrawi G., H. Salaheldin, M. Abdelghany, (2021), Structural investigations on inorganic $Al_2O_3–ZnO$ composites, *J. Appl. Phys.*, **127**, 1-6.

15. El Damrawi G., A. Behairy, R. Atef, (2019), Structural characterizations for glass ionomer cement doped with transition metal phthalocyanines, *NJGC*, **9**, 67-80.

16. El-Damrawi G., A. Behairy, A.m. Abdelghan, (2018), Structural characterization of novel cerium phosphate glass ionomer cements (GICs) doped with GaCl (Phthalocyanine), *NJGC*, **8**, 23-39.

17. Malavasi G., A. Pedone, M.C. Menziani, (2013), Study of the structural role of gallium and aluminum in 45S5 bioactive glasses by molecular dynamics simulations, *J. Phys. Chem.*, **117**, 4142−4150.

18. Phillips M.W., G.V. Gibbs, P.H. Ribbe, (1974), The crystal structure of danburite: A comparison with anorthite, albite, and reedmergnerite, Am Min, **59**, 79-85.

19. Phillipsi M.W., A.A. Colville, P.H. Ribbe, (1971), The crystal structures of two oligoclases: A comparison with low and high albite, Z. Kristallogr. *Cryst. Mater.*, **133**, 43-65.